Geotechnical Engineering Journal of SEAGS & AGSSEA

https://ph01.tci-thaijo.org/index.php/seags_agssea_journal

Strength and Durability of Quartzite from the Pandrang and the Chisapani Quartzite Units of Bhimphedi Group, Central Nepal Lesser Himalaya

A. Dinesh Raj Sharma[1] and B. Naresh Kazi Tamrakar[2]
[1]*Department of Geology, Tribhuvan University, Kathmandu, Nepal*
[2] *Associate Professor of Department of Geology, Tribhuvan University, Kathmandu, Nepal*
Corresponding E-mail: *naresh.tamrakar@cdgl.tu.edu.np*

ABSTRACT: This study focuses on the characterization and evaluation of quartzites sourced from the Pandrang Quartzite and the Chisapani Quartzite belonging to the Bhimphedi Group of the Lesser Himalayan sequence for their potential use as railway aggregates. The objective of the research is to assess the physical, mechanical, and durability properties of these crushed rock aggregates, considering their suitability for railway applications. The quartzites, classified as medium-grained, monomictic quartzites belonging to the Precambrian Age, exhibit white to yellowish or brownish white colour, and rough surface texture. The investigation gives away consistent and similar physical properties in both quartzite samples, including narrow ranges in density, specific gravity, and water absorption. While the quartzites demonstrate varying levels of strength, with a majority falling into the strong to very strong category, some exhibit medium strong and extremely strong characteristics. Additionally, the aggregates show a range of values for the Aggregate Impact Value (AIV) and Aggregate Crushing Value (ACV), indicating variations in toughness. The quartzites show high resistance to slaking, minimal weight changes during slake durability testing, and superior resistance to freeze and thaw weathering. Moderate hardness and abrasion resistance suggest their suitability as durable aggregates for ballast. Despite comparable density ranges and aggregate crushing values, the Pandrang Quartzite generally exhibits higher strength and durability than the Chisapani Quartzite, suggesting superior quality. Except for crushing resistance, the quartzites meet the requirements specified by (American Railway Engineering and Maintenance-of-Way Association (AREMA) and British Railway Standards, making them suitable for railway applications. The study provides valuable insights into the physical, mechanical, and durability characteristics of quartzite aggregates, guiding their potential utilization in railway infrastructure with an emphasis on durability and strength.

KEYWORDS: Quartzite Characterization, Railway Aggregates Evaluation, Durability Assessment for Railway Applications.

1. INTRODUCTION

Railway tracks are one of the essential and suitable means of transport for the socio-economic and industrial growth of the nation. The railway transport network is a priority of Nepal's transport system (Thapa, 2018; Chitrakar, 2021). Considering this, ahuge amount of railway track ballasts will be required in the future. The demand for ballast can be fulfilled from resources of quartzites from the Central Nepal Himalaya.

Various types of ballasts are used in railway tracks and are derived by crushing hard stones like granite, quartzite, and sandstone (Mundrey, 2009). Quartzite is stiff and durable among the rock types, and it is best for ballast. Quartzite ballasts often have good stiffness, long-term durability, and frictional resistance among the rock types (Hamnett, 1943). Various researchers have studied physical, mechanical, and durability properties to assess rocks for ballasts (Indraratna et al., 2006; Kolay and Kayabali, 2006; Guo and Jing, 2017; Guo et al., 2018). Rock types with higher specific gravity, hardness, and resistance to weathering are considered good for ballasts (Kolay & Kayabali, 2006).

The Point-load Strength Index (PLSI), Aggregate Crushing Value (ACV), and Aggregate Impact Value (AIV) are crucial parameters for evaluating the quality of ballasts. The Point-load Strength Index measures the individual particle strength and resistance to deformation, indicating the material's ability to withstand concentrated loads. The ACV assesses the resistance of the ballast to crushing under gradual compressive loads, ensuring its structural integrity and preventing particle breakdown. The AIV evaluates the ballast's ability to withstand sudden impacts without excessive fragmentation. When the strength properties of the ballasts are unsound, the railway ballasts break, diminishing load-bearing capacity and, finally, the performance of the track.

Likewise, the durability of ballasts is also a crucial property to be tested for rocks. Slake durability is among the important properties in evaluating the deterioration of rocks under cyclic wetting and drying environment (Franklin & Chandra, 1972; Brown, 1981; Dick & Shakoor, 1995); therefore is evaluated for ballasts because the latter should withstand against such weathering environment. Los Angeles Abrasion Value (LAAV) and Sulphate Soundness Value (SSV) are among the durability values thatare determined to evaluate the material's resistance to wear and impact and to degradation under freeze and thaw weathering environments. Raymond (1985) emphasized the Los Angeles Abrasion test and grading of ballast and concluded that evaluation of ballast requires aggregate selection and monitoring. Ballasts are tested to determine durability properties and ensure the long-term durability of ballasts on the track.

Bista and Tamrakar (2015) studied the strength and durability of rock aggregates from the Lesser Himalaya and concluded that quartzites, siliceous dolomites, and psammitic schists were more suitable for construction aggregates compared to slate, phyllite, metasandstone, and gneiss. Quartzites possess various characteristics in composition, microfabrics, physical properties, strength and durability (Abdullah & Singh, 2010). Variations in strength and durability among quartzites are often related to their intrinsic properties (Gupta & Sharma, 2012; Paudel & Tamrakar, 2012; Bista & Tamrakar, 2015). That is why the study of the properties of ballast is crucial, and the strength and durability properties of ballast will help to determine whether the ballast is appropriate. Therefore, the main objective of this study is to determine the physical, mechanical and durability of quartzite ballasts from two different stratigraphic units of the Bhimphedi Group of the Lesser Himalaya.

https://doi.org/10.14456/seagj.2025.3 Published on 17 July 2025

2. GEOLOGICAL SETTING OF RESEARCH AREA

The study area is located in the Makawanpur District, along the area between Suparitar and Bhimphedi (Figure 1). The area has access routes to the Tribhuvan Rajpath and the Bhimphedi-Bhainse road section of the study site. The study site lies in the Lesser Himalaya of the Central Nepal Himalayas (Figure 2). This area is located in the southernmost limb of the Mahabharat Synclinorium. Three formations of the Upper Nawakot Group (Table 1) are exposed north of the Main Boundary Thrust (MBT) in the hanging wall. The Bhimphedi Group and the Upper Nawakot Group are separated by the Mahabharat Thrust (MT) (Stöcklin & Bhattarai, 1977; Stöcklin, 1980) along which the Bhimphedi Group thrusts over. The formations of the Bhimphedi Group are deformed to a large plunging syncline. The Precambrian Bhimphedi Group, consisting of relatively high-grade metasediments, shows a gradual decrease in the metamorphic grade from garnet schist at the bottom to the sericite-chlorite grade at the top. The metamorphic grade is relatively high along the MT. Two stratigraphic units of the Bhimphedi Group; namely the Pandrang Quartzite member of the Kalitar Formation, and the Chisapani Quartzite contains predominantly outcrops of quartzite beds (Table 1), which extend NW-SE dipping towards NE.

3. METHODOLOGY

Stratified selective samples of quartzites were taken as grab samples from the quartzite beds of the Pandrang Quartzite (Member of the Kalitar Formation) and the quartzite beds of the Chisapani Quartzite exposed at the portion of the Hetauda to Bhimphedi section. Sampling horizons and lithology were recorded during sampling. The required number of samples were brought to the material testing laboratory for petrography and further tests. Test samples from the individual samples were prepared for desirable tests: physical, mechanical, and durability properties.

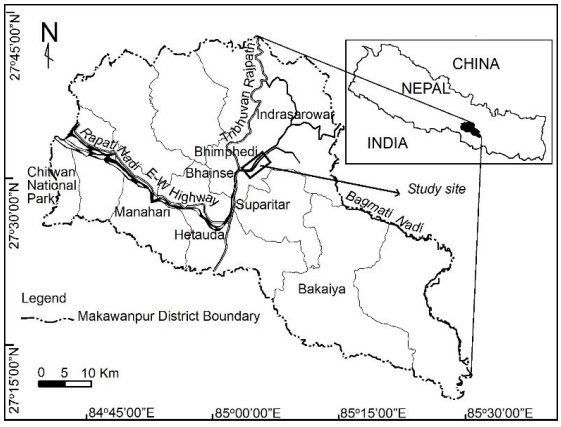

Figure 1 Location map of the study area

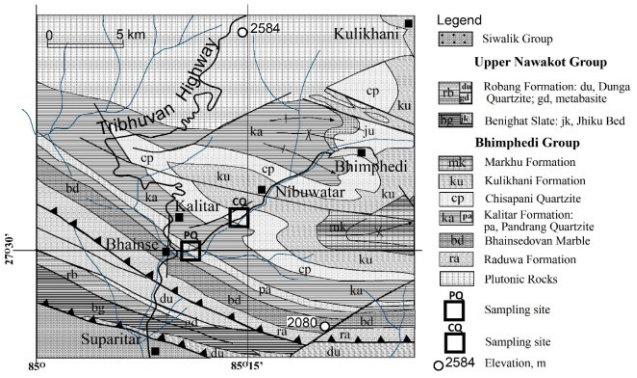

Figure 2 Regional geology and location of sampling sites

3.1 Tests for Physical Properties

The laboratory procedures for density and water absorption were followed according to (ASTM, C127 2011). The test sample was oven-dried at constant mass at a temperature of 110±5°C, and the oven-dry (OD) mass of the sample was recorded. Subsequently, the sample was immersed in water at room temperature for 24 hr. Then the sample's saturated surface dry (SSD) mass of the sample was recorded. The SSD sample was then immersed in water, removing all entrapped air by shaking the container. The apparent mass of the sample was measured in water. The following equations were used to compute density of oven dried sample (D), specific gravity (G) and water absorption (WA).

$$D = 997.5\frac{A}{(B-C)} \quad (1)$$

$$G = \frac{A}{(B-C)}.100 \quad (2)$$

$$WA = \frac{(B-A)}{(A)}.100 \quad (3)$$

where A is the mass of the oven-dried test sample in the air (in grams), B is the mass of the saturated- surface-dry test sample in the air (grams), and C is the apparent mass of the saturated test sample in water (grams).

Bulk density takes into accountboth aggregates and void spaces in a given volume. It is also a measure of how well-packed the aggregates are in the given space. The bulk density of ballasts was determined (ASTM, 2006) by rodding the ballast in a measure. The dry Bulk density for rodding was calculated using the following relation:

$$BulkDensity = \frac{(G-T)}{(V)} \quad (4)$$

where G is the oven-dry mass of the sample plus the measure (kg), T is the mass of the measure (kg), and V is the volume of the measure (m^3).

3.2 Test for Mechanical Properties

Tables should be presented as indicated in Table 1. Their layout should be consistent throughout. Horizontal lines should be placed above and below label headings, below subheadings, and at the end of the table. Vertical lines should be avoided.

The point load strength index (PLSI) test, which was originally introduced by Broch and Franklin (1972), was conducted using irregular lumps following the procedure of (ASTM, 2002). Irregular lumps were loaded normally to the stratification, and the breakage load was recorded in KN. The PLSI was calculated using the following equation:

$$I_s = \frac{P}{(De^2)} \quad (5)$$

where I_s is PLSI, P is a failure load (KN), and De is the equivalent core diameter (m).

The equivalent core diameter was calculated using the following expression:

$$De^2 = \frac{4A}{\pi} \quad (6)$$

where A is a minimum cross-sectional area of the plane through the platen contact points and was obtained from the products of average width and average thickness of the lump measured. The standard point load strength index, $I_{s(50)}$ was obtained using the following expression:

$$I_{s(50)} = \left(\frac{D_e}{50}\right)^{0.45} I_s \quad (7)$$

where $(De/50)^{0.45}$ is a size correction factor.

For classification of strength of intact rocks, uniaxial compressive strength (UCS) was calculated by applying the following relation after (ASTM, 2002):

$$UCS = 24I_{s(50)} \quad (8)$$

For determining AIV, the aggregate test sample of size between 12.5 mm and 9.5 mm and weight of about 500 g was prepared according to BSI (1990a) and was filled in a cylindrical holder, one-third at a time and tamped 25 times with a tamping rod. The test sample was then fixed in the impact machine. The test sample was subjected to a total of 15 blows by the 14 Kg weight of the hammer, each being delivered at an interval of not less than one second. The crushed aggregate was then removed and sieved on the 2.36 mm sieve. AIV was calculated using the following expression:

$$AIV = \frac{M_1 - M_2}{M_1}.100 \quad (9)$$

where M_1 is the initial weight of the aggregate sample, and M_2 is the weight of aggregate retained on a 2.36-mm sieve after the test. The aggregate crushing value (ACV) provides a relative measure of resistance to crushing under a gradually applied compressive load. About 3 kg of aggregate test samples of size between 12.5 mm and 9.5 mm were filled in the sample holder, one-third at a time, by tamping 25 times (BSI, 1990b). The sample holder with the test sample was fixed in a compression machine and was gradually loaded between platens to achieve 400 KN at 15 minutes. The ACV was calculated by using the following expression:

$$ACV = \frac{W_1 - W_2}{W_1}.100 \quad (10)$$

where W_1 is the initial weight of the dry sample, and W_2 is the weight of the aggregate retained on a 2.36 mm sieve after the test.

3.3 Durability Test

The durability of rocks against cyclic wetting in water and drying is measured by the Slake Durability Index (SDI). ASTM (2008) was followed to carry out an SDI test to report standard SDI at second cycles, I_{d2}. Furthermore, three more cycles were added to see the deterioration behaviour of samples. Therefore, a total of five-cycle tests were adopted. Thus, the natural water content before the SDI test was calculated using the following expression:

$$W = \frac{A - B}{B}.100 \quad (11)$$

where W is the percentage of water content, A is the mass of the sample at the natural moisture content (g), and B is the mass of the oven-dried sample before the first cycle (g).

The I_{d2} was computed as follows:

$$I_{d2} = \frac{W_2}{B}.100 \quad (12)$$

where I_{d2} is slake durability index (second cycle), B is the mass of oven-dried sample before the first cycle in grams, and W_2 is the mass of oven-dried sample retained after the second cycle, in grams. Similarly, the SDI in each of the successive individual cycles was computed. For assessing disintegration behaviour, samples at two stages were tallied with Type 1, Type 2, and Type 3 patterns.

Los Angeles Abrasion test measures the resistance of aggregates to abrasion and impact and is an indirect test of the hardness of rock. The test was carried out in an LAA machine according to ASTM (2009). To conduct the LAA test, the Grade A test sample that constituted 5 kg of each mass of aggregate of 50 mm down to 37.5 mm size and that of 37.5 mm down to 25 mm size was prepared and was placed in the LAA machine along with 12 steel balls. The machine revolved for 1000 revolutions. After completion of revolutions, the steel balls were taken out, the sample was place in a tray, and was sieved at 1.7 mm sieve. The retained sample was weighed. The following formula was used to calculate the abrasion loss in percentage:

$$LAAV = \frac{(W_1 - W_2)}{W_1}.100 \quad (13)$$

where LAAV is the Los Angeles Abrasion Value, W_1 is the initial weight of the sample, and W_2 is the weight of the sample retained on a 1.7 mm sieve.

The sulphate soundness test was carried out on the aggregate samples to determine the durability of aggregate against physical weathering. The test was done as per the standard procedure of determining the sulphate soundness of aggregates as ASTM (2005). Sulphate soundness value (SSV) expressed in percentage was calculated as,

$$SSV = \frac{(W_1 - W_2)}{W_1}.100 \quad (14)$$

where, W_1 is an initial weight of sample (kg) and W_2 is the weight of the sample after five cycles.

4. RESULTS AND DISCUSSIONS

4.1 Geological Outlines

The study site, which is located along the Suparitar-Bhimphedi-road, constitutes two major quartzite units, the Pandrang Quartzite and the Chispani Quartzite, across the Bhimphedi Group of the Kathmandu Complex. The Pandrang Quartzite is a member of the Kalitar Formation, which is dominated by mica schist and quartzite (Figure 3). The formation is underlain and overlain, respectively, by the Bhaisedovan Marble and the Chisapani Quartzite. The Chispani Quartzite dominantly comprises white quartzite and subordinately of schist (Figure 4) and is underlain by the Kalitar Formation and overlain by the Kulekhani Formation. Both units extend NW-SE, and dip towards NE, and form the southern limb of the broad NW-plunging syncline.

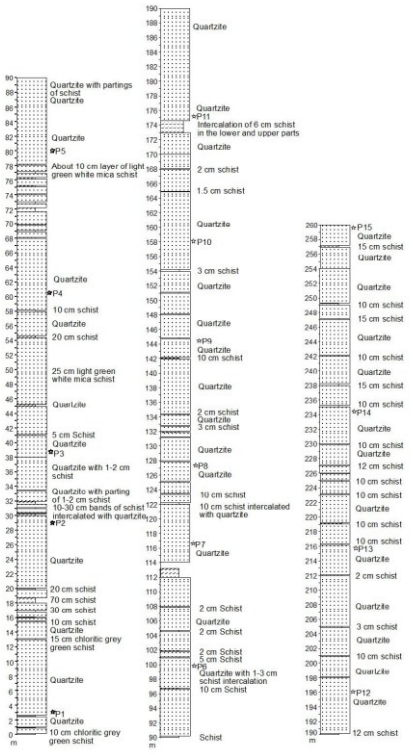

Figure 3 Graphic log of the Pandrang Quartzite along a tributary contributing to the Rapati Nadi at Suparitar-Bhimphedi road. P1 to P15 are sample numbers

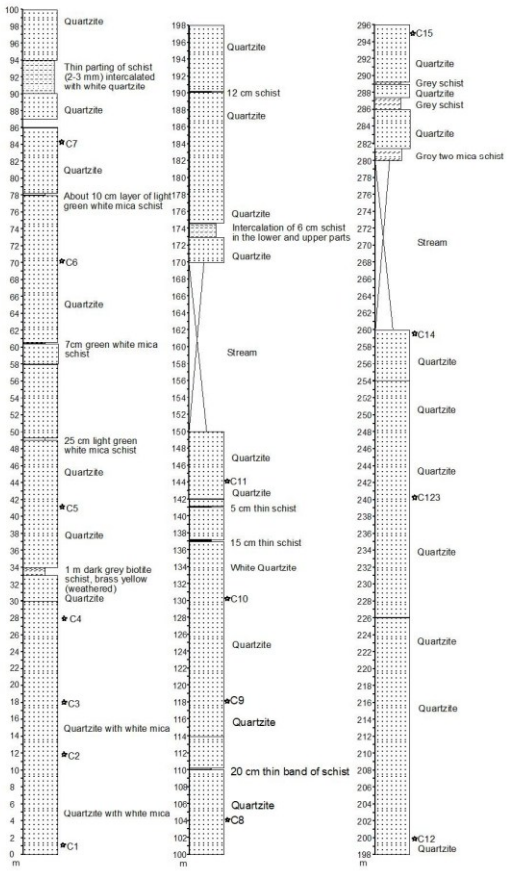

Figure 4 Graphic log of the Chisapani Quartzite along the Rapati Nadi near Nibuwatar. C1 to C15 are sample numbers

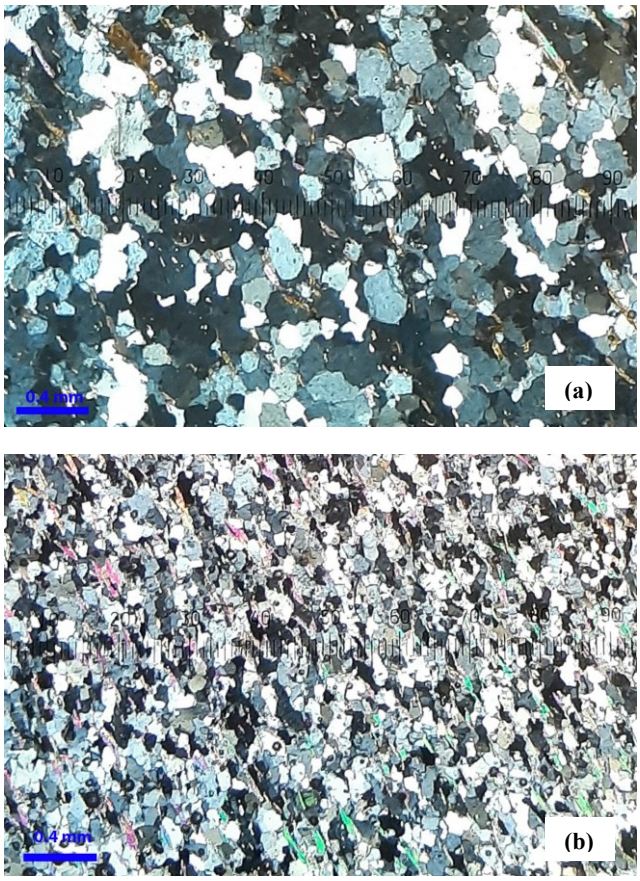

Figure 5 Photomicrographs in crossed polarized light, showing fabric and composition of quartzites from two stratigraphic units. (a) Pandrang Quartzite and (b) Chisapani Quartzite

4.2 Description and Classification of Samples

The ballasts were described and classified considering three attributes, i.e., aggregate type, physical properties, and petrological characteristics (Table 2). Samples from both the Pandrang Quartzite and the Chisapani Quartzite are crushed rocks sourced from quartzite bedrocks of the Precambrian age (Stöcklin & Bhattarai, 1977; Stöcklin, 1980). They have a nominal size of 37.5 mm, a rough surface texture, and are very angular, bladed to prolate shape, and white to yellowish or brownish white colour. Coating and extraneous materials are absent. These samples are classified as medium-grained monomictic Quartzite.

4.3 Petrography of Quartzites

Quartzites from the Pandrang Quartzite are medium-grained, having a microstructure of pervasive tectosilicate domains with discontinuous foliation domains as defined by muscovite and biotite (Figure 5a). Quartz content is 83-95%, and only a few quartzites have 1% feldspar. Phyllosilicates are composed of sericite exceeding muscovite, and some quartzites have biotite up to 5% (Table 3).

Quartzites from the Chisapani Quartzites are medium-grained with pervasive tectosilicate domains and foliation defined by muscovite, sericite, and biotite (Figure 5b). The foliation is discontinuous and wavy. The constituent minerals are quartz of 85-91%, subequal muscovite (3-6%) and sericite (3-5%), biotite varying from 1 to 6%, and opaque heavies between 1 and 3% (Table 3). Based on mineral constituents, both quartzites belong to regional metamorphic environments and are of biotite grade. Quartzites from the Chisapani Quartzite have slightly larger quartz grains, more distinct muscovite foliation, and more frequent biotites than those of the Pandrang Quartzite.

4.4 Physical Properties

4.4.1 Density, Specific Gravity, and Water Absorption

The Pandrang Quartzite samples exhibit oven-dry densities ranging from 2567 to 2693 kg/m^3 (Table 4). The specific gravity (relative density) varies between 2.51 and 2.68. The Chisapani Quartzite samples display oven-dry densities ranging from 2521 to 2733 kg/m^3, and specific gravity ranging from 2.53 to 2.75. Density does not rely on quartz content in this study, which is opposed to the result of increasing density with an increased amount of quartz obtained by Gupta and Sharma (2012) for quartzites from the northwest Himalayas. The quartzites studied by Gupta and Sharma (2012) were of medium- to coarse-grained, sillimanite grade with highly preferred orientation of grains, whereas the quartzites from the Pandrang and the Chisapani Quartzites are of biotite grade.

Water absorption (WA) determines the ability of an aggregate to absorb water in a moist environment and does indicate the connectivity of voids from the surface inwards of the particles. The water absorption values of the samples from the Pandrang Quartzite range from 0.24 to 0.74%. Similarly, Water absorption values of the samples from the Chisapani Quartzite range from 0.24% to 1.00%. The samples thus show relatively narrow ranges of density and specific gravity water absorption values, indicating consistent physical properties. Despite this, the WA of the samples from the Chisapani Quartzite are more compared to those from the Pandrang Quartzite.

Density of the Pandrang Quartzite and the Chisapani Quartzite studied at present comes to vary within a comparable range compared to the earlier studies (Abdullah & Singh, 2010; Paudel & Tamrakar, 2012; Gupta & Sharma, 2012; Bista & Tamrakar, 2015; Singh et al., 2017). Specific gravity and water absorption are also quite comparable with the results of the previous studies (Abdullah & Singh, 2010; Paudel & Tamrakar, 2012; Adom-Asamoah et al., 2014; Bista & Tamrakar, 2015) of similar and different quartzites.

4.4.2 Bulk Density

Bulk density includes both void spaces among aggregate particles and the density contributed by particles. In the case of the sample from the Pandrang Quartzite, the bulk density values ranged from 1152 to 1348 kg/m³ (Table 5). Higher bulk density indicated a denser article arrangement. The percentage of voids ranged from 48% to 56% in the samples from the Pandrang Quartzite, with lower percentages indicating a more compact structure and higher percentages suggesting greater porosity. Samples with higher bulk densities generally exhibited lower percentages of voids, indicating a denser and less porous structure, while samples with lower bulk densities tended to have higher percentages of voids, suggesting a looser and more porous structure. Therefore, the bulk density of the samples depends on the arrangement of particles in a container.

4.5 Mechanical Properties

4.5.1 Point Load Strength Index

The point load strength index (PLSI) determines the strength index value at the given point. The quartzite samples are moderately strong to extremely strong, and the majority are strong to very strong, according to the International Society of Rock Mechanics (Brown 1981). The maajority of samples from the Pandrang Quartzite are classified as "very strong" with high UCS values ranging from 70 to 207 MPa (Table 6). These results indicate variations in the strength of the Pandrang Quartzite samples, with some demonstrating very high strength and the ability to withstand significant compressive loads. Similarly, samples from the Chisapani Quartzite give UCS ranging from 25 to 337 MPa, which fall in “medium to extremely strong” categories. Several samples are classified as "strong" and "very strong" indicating their varying levels of compressive strength. Samples are classified as "strong" and "very strong" indicating their varying levels of compressive strength.

Point-load strength index and computed UCS of the samples from the Pandrang Quartzite and the Chisapani Quartzite vary within a wider range compared to the results of the similar Quartzite from western areas in the earlier studies (Bista & Tamrakar, 2015). The majority of quartzites gave UCS less than 150 MPa except for higher values of around 300 MPa, as given by Adom-Asamoah et al. (2014).

4.5.2 Aggregate Impact Value

The aggregate impact value (AIV) is a measure of resistance to sudden impact, which may differ from its resistance to gradually applied compressive load. In short, it is a measure of the toughness of rock material. Samples from the Pandrang Quartzite and the Chisapani Quartzite give AIV of 13-24 % and 14-34%, respectively (Table 7). The AIV does not differ from the AIV of other quartzites, as reported by Adom-Asamoah et al. (2014), who obtained as low as 8%. AIV of quartzites from the Pandrang Quartzite is relatively lower than that of the Chisapani Quartzite. The majority of the samples from the Chisapani Quartzite possess AIV exceeding 20%, showing that the quartzites from the Chisapani Quartzite are less resistant to impact stress compared to the quartzites from the Pandrang Quartzites.

4.5.3 Aggregate Crushing Value

The aggregate crushing value (ACV) provides a relative measure of the resistance of an aggregate to crushing under a gradually applied compressive load. Samples from the Pandrang Quartzite the ACV values of samples from the Pandrang Quartzite and the Chisapani Quartzite range from 21 % to 30% and from 20 to 38 %, respectively (Table 7). Two Samples from the Pandrang Quartzite have relatively high ACV values (30%); otherwise the majority of the samples have ACV <25%, indicating relatively high resistance to crushing. On the other hand, five samples from the Chisapani Quartzite have ACV values exceeding 30% and the remaining ten samples have ACV values between 20 and 30%, indicating that the resistance to crushing is optimal. ACV of the current study is similar to that of quartzites from other areas studied by Paudel and Tamrakar (2012) and Adom-Asamoah et al. (2014)

4.6 Durability

Three durability attributes, i.e., slake durability index (I_{d2}), Los Angeles Abrasion value (LAAV), and sulphate soundness value (SSV), were determined to assessthe durability against slaking, abrasion, and freeze and thaw of quartzites respectively.

4.6.1 Slake Durability Index

The slake durability index is a weathering test that determines the resistance to slaking under cyclic wetting and drying. The test result of the Pandrang Quartzite indicates that the second-cycle slake durability index, I_{d2}, ranges from 99 % to 100% with deterioration type I (Figure 6), i.e., all the ten pieces of the test samples were intact and retained after the second cycle (Table 8). The SDI of all the samples is classified as very high durability based on Goodman (1980). The fifth-cycle SDI, I_{d5}, of all the samples ranges from 98 % to 100%, showing no significant change occurring up to the fifth cycle.

The samples from the Chisapani Quartzite exhibit I_{d2} varying between 98 and 100%, classified as very high durability, and undergoing deterioration type I (Figure 6; Table 7). The fifth-cycle SDI varies from 97 to 100%, thus showing no remarkable change from the second to the fifth cycle, except for a few sample whose durability was deduced from very high durability to high durability.

Figure 6 Samples under slake durability test showing type I deterioration. (a) samples from the Pandrang Quartzite after the second cycle, samples from the Pandrang Quartzite after the fifth cycle, (c) samples from the Chisapani Quartzite after the second cycle, and (d) samples from the Chisapani Quartzite after the fifth cycle

4.6.2 Los Angeles Abrasion Value

The LAA test determines the hardness property of aggregates. It measures the abrasion resistance of aggregates (ASTM, 2009).

LAAV of the samples from the Pandrang Quartzite varies between 23 and 37%, whereas those from the Chisapani Quartzite are between 22 and 49% (Table 9). The majority of the samples exhibit a high range of hardness and abrasion resistance. Few samples from the Chisapani Quartzite show higher values (>40%).

All the quartzite particles tested were of angular to subangular shape because all the samples were crushed aggregate. However, with the increased roundness of fresh ballasts, the degree of Los Angeles abrasion tends to decrease (Okonta, 2015). This is as opposed to the results of (Guo et al., 2018). They found flaky and elongated particles to be worn out more readily, losing the volume of particles under the abrasion test. But in the present study, quartzites were less flat and slightly elongated; even under this circumstance, aggregate form does not have much bearing on durability against abrasion, presumably due to good interlocking of grains in quartzites. Sekine et al. (2005) also indicated that relationships between shape and strength diminish as the stiffness of ballasts increases. The majority of the samples fall into the acceptable limit of <35% suggested by AREMA (2010).

4.6.3 Sulphate Soundness Value

Sulphate Soundness is a cyclical test that evaluates aggregates for durability and resistance to degradation from weather cycles in freeze and thaw environments. The samples from the Pandrang Quartzite and the Chisapani Quartzite show very low Sulfate Soundness Values (SSV) of respectively 0-0.25% and 0-0.75% (Table 10). This indicates that the quartzite samples possess very high resistance to weathering due to freezing and thawing under repeated cycles. The low SSV can be attributed to the negligible volume of effective pores in the quartzite samples that prevent sulphate fluid from penetrating the samples.

4.7 Comparison with Specification

The comparison between quartzite from the Pandrang Quartzite and the Chisapani Quartzite with the existing AREMA (2010) and BS EN 13450 (BS 2013) reveals several similarities and differences. When it comes to physical properties, both quartzites have similar density ranges that fall within the specified limits set by the standards (Table 11). Both quartzite samples demonstrate relatively low water absorption. The water absorption percentages for both quartzites are also comparable and lie within the acceptable range of AREMA (2010). The quartzites from the Chisapani Quartzite exhibit a slightly higher range of bulk density, 1260-1441 kg/m^3, compared to samples of the Pandrang Quartzite, i.e., 1152-1371 kg/m^3. The bulk density is attributed to particle shape and their packing in the container. The bulk density of quartzites from both Pandrang and the Chisapani units the lies under acceptable limit defined by AREMA (2010).

In terms of mechanical properties, the samples from the Pandrang Quartzite show narrower range of UCS (70 to 207 MPa) compared to those of the Chisapani Quartzite (25 MPa to 337 MPa) (Table 7). When considering the AIV, quartzites from the Pandrang Quartzite vary in a narrower range (13% to 24 %) compared to those of the Chisapani Quartzite (19% to 34%) (Table 8). According to BS (2013), this range should be less than 22%. Two samples from the Pandrang Quartzite and eight samples from the Chisapani Quartzite exceed this range. Similarly, both quartzites have similar ranges of ACV (21-30%) (Table 8). Except for a few samples, the majority of the samples from both units exceed the range of 22% of BS (2013). Hence, in terms of compressive strength, except for a few quartzites from the Chisapani Quartzite, the rest are strong to extremely strong and lie within specified limits. In terms of impact and crushing strengths, quartzites from the Pandrang Quartzite show better results than that from the Chisapani Quartzite.

Considering durability, quartzites from both geological units demonstrate excellent slake durability, with the Pandrang Quartzite ranging from 98% to 100% and the Chisapani Quartzite ranging from 97.20% to 100%. However, there are some differences in the range of LAAV. Quartzite from the Pandrang Quartzite has a narrower range (21-30%) than those from the Chisapani Quartzite (22-49%) (Table 10). Additionally, one sample from the Pandrang Quartzite and four samples from the Chisapani Quartzite exceed the 35% limit of AREMA (2010). Hence, the majority of quartzites give LAAV below the limiting value, showing that those quartzites are appropriate for ballasts. If the LAAV of quartzites is compared with BS (2013), the majority of quartzite does not meet the specified LAAV. In terms of sulfate soundness, quartzites from both geological units demonstrate low sulphate soundness values lying in the narrow range and within the threshold, <5% of AREMA (2010), thus exhibiting high resistance of quartzites to freeze and thawing.

In conclusion, the comparison shows that quartzites from both the Pandrang Quartzite and the Chisapani Quartzite (Table 11) in majority meet the shape index, physical property, mechanical property, and durability requirements set by the AREMA (2010) and BS EN 13450 (BS 2013), except for crushing strength in case of the Pandrang Quartzite, and both crushing and impact strengths in crushing strengths in case of the Chisapani Quartzite. However, there are some variations in specific properties, such as LAAV, where Chisapani Quartzite exhibits a wider range. These findings provide valuable insights for considering the suitability of Quartzite to the railway applications.

5. CONCLUSIONS

Quartzites from the Pandrang Quartzite and the Chisapani Quartzite are crushed rocks sourced from bedrock with rough surface texture and colors ranging from white to yellowish or brownish white. They are classified as medium-grained monomictic quartzites that belong to the Precambrian Age,

Both quartzite samples show consistent and similar physical properties, as indicated by their relatively narrow ranges in density, specific gravity, and water absorption.

Quartzites demonstrate varying levels of strength, with a majority categorized as strong to very strong, and some samples exhibiting medium strong and extremely strong. They exhibit a range of values for the AIV and ACV with some samples showing better resistance to impact and crushing. Overall, the results suggest variations in the toughness of the quartzite aggregates.

Quartzites demonstrate high resistance to slaking, minimal weight changes during slaking durability testing, and high resistance to freeze and thaw weathering.

Quartzites exhibit moderate hardness and abrasion resistance, indicating their suitability as durable aggregates for ballast.

Both quartzites demonstrate low water absorption, comparable ranges of density and aggregate crushing value. Quartzites from the Pandrang Quartzite generally exhibit higher strength and durability compared to those from the Chisapani Quartzite and therefore are of superior quality.

Except for crushing resistance, quartzites result in good physical properties, strength and durability, which meet the requirements specified by the AREMA (2010). But compared to the British Railway standards (BS, 2013), the quartzites perform well except for crushing strengths.

6. ACKNOWLEDGEMENT

Authors are thankful to Department of Mines and Geology, Nepal, Institute of Engineering, Pulchowk, and Central Department of Geology, Kirtipur, Nepal for providing laboratory facilities. Authors thank J. Gurung, S. Ranabhat, D. Shrestha, S. Maharjan, and S. Pradhanang for their helping hands during sample collection and laboratory analysis. Authors are thankful to M. Shrestha for graphics.

7. REFERENCES

Abdullah, H., and Singh, S., (2010). “Laboratory evaluation of Five Quartzites.” *In Proc. Indian Geotechnical Conference, IGS Mumbai Chapter and IIT Bombay, GEOtrendz*, pp. 263-266.

Adom-Asamoah, M., Tuffour, Y. A., Afrifa, R. O., and Kankam, C. K., (2014). “Strength Characteristics of Hand-quarried Partially-

weathered Quartzite Aggregates in Concrete." *American Journal of Civil Engineering,* v. 2(5), pp. 134-142.

AREMA, (2010). "Manual for Railway Engineering, Ch. 1: Roadway and Ballast." *American Railway Engineering and Maintenance of Way Association (AREMA).,* v. 1, pp 1-10.

ASTM, (2002). "Standard Test Method for Determination of the Point Load Strength Index of Rock and Application to Rock Strength Classifications." *D-5731. ASTM International, West Conshohocken, PA, USA.,* v. 4(2), pp.1-9.

ASTM, (2005). "Standard Test Method for Soundness of Aggregates by Use of Sodium Sulfate or Magnesium Sulfate." *ASTM C88-05. In: ASTM International West Conshohocken, PA, USA.,* v. 4(2), pp. 1-10.

ASTM, (2006). "Standartd Test Method for Bulk Density ("Unit Weight") and Void in Aggregate." 29/C 29M–97 (Reapproved 2003). *ASTM International, West Conshohocken, PA, USA.,* v. 4(2), pp. 1-7.

ASTM, (2008). "Standard Test method for Slake Durability of Shales and Similar Weak Rocks (ASTM D4644–08)." *Annual of ASTM Standards, West Conshohocken, PA,* v. 4, pp. 880-882.ASTM, (2009). "Standard Test Method for Resistance to Degradation of Large Size Coarse Aggregate by Abrasion and Impact in the Los Angeles Machine." *C535-09. ASTM International, West Conshohocken, PA, 2009,* v. 4(2), pp.1-6.

Bista, K., and Tamrakar, N. K., (2015). "Evaluation of Strength and Durability of Rocks from Malekhu-Thopal Khola Area, Central Nepal Lesser Himalaya for Construction Aggregates." *Bulletin of Department of Geology, v. 18,* pp.15-34.

Broch, E., and Franklin, J., (1972). "The Point-load Strength Test." *International Journal of Rock Mechanics and Mining Sciences. v. 9,* pp. 669-697.

Brown, E. T., (1981). "Rock Characterization, Testing and Monitoring: ISRM Suggested Methods." *ISRM Suggested Methods Oxford Pergamon Press, v.1,* p. 211.

BSI, (1990a). "Methods for Determination of Aggregate Impact Value (AIV)." *British Standard Institution (BSI), BS 812–112,* pp. 1-8.

BSI, (1990b). "Methods for Determination of Aggregate Crushing Value (ACV)." *British Standard Institution (BSI), BS 812-110,* pp.1-10.

BS, (2013). "Aggregate for Railway Ballast." *British Standard Institution BS EN 13450,* pp.1-38.

Dick, J. C., and Shakoor, A., (1995). "Characterizing Durability of Mudrocks for Slope Stability Purposes." *Geol Soc Am Rev Eng Geol X, v. 5,* pp. 121-130.

Franklin, J. A., and Chandra, R., (1972). "The Slake-durability Test." *International Journal of Rock Mechanics and Mining Sciences & Geomechanics Abstracts, Elsevier v. 9(2),* pp. 181-188.

Guo, Y., and Jing, G., (2017). "Ballast Degradation Analysis by Los Angeles Abrasion Test and Image Analysis Method." *The 10th International Conference on the Bearing Capacity of Roads, Railways and Airfields (BCRRA 2017), Athens, CRC Press,* pp. 283-288.

Guo, Y., Markine, V., Song, J., and Jing, G., (2018). "Ballast Degradation: Effect of Particle Size and Shape Using Los Angeles Abrasion Test and Image Analysis." *Construction and Building Materials, v. 169,* pp. 414-424.

Gupta, V., and Sharma, R., (2012). "Relationship between Textural, Petrophysical and Mechanical Properties of Quartzites: a Case Study from Northwestern Himalaya." *Engineering Geology, v. 135,* pp. 1-9.

Hamnett, R. A., (1943). "British Railway Track: Design, Construction and Maintenance." *The Institution of Permanent Way Engineers, v.112-114,* pp 1-126

Indraratna, B., Khabbaz, H., Salim, W., and Christie, D., (2006). "Geotechnical Properties of Ballast and the Role of Geosynthetics in Rail Track Stabilization." *Proceedings of the Institution of Civil Engineers-Ground Improvement, v. 10(3),* pp. 91-101.

Kolay, E., and Kayabali, K., (2006). "Investigation of the Effect of Aggregate Shape and Surface Roughness on the Slake Durability Index Using the Fractal Dimension Approach." *Engineering Geology, v. 86(4),* 271-284.

Mundrey, J., (2009). "Railway Track Engineering." *McGraw-Hill Education. 5th edition,* ISBN: 978-0-07-161477-1, 824p.

Okonta, F., (2015). "Effect of Grading Category on the Roundness of Degraded and Abraded Railway Quartzites." *Engineering Geology, v. 193,* pp. 231-242.

Paudel, P. N. and Tamrakar, N.K., (2012). "Geology and Rockmass Condition of Dhulikhel-Panchkhal Area, Kavre District, Central Nepal Lesser Himalaya." *Bulletin of Department of Geology, v.15,* pp. 1–14.

Raymond, G. P., (1985). "Research on Railroad Ballast Specification and Evaluation." *Transportation Research Record, v. 1006,* pp. 1-8.

Sekine, E., Kono, A., and Kito, A., (2005). "Strength and Deformation Characteristics of Railroad Ballast in Ballast Particle Abrasion Process." *Quarterly Report of RTRI, v. 46(4),* pp. 256-261.

Singh, T., Jain, A., and Rao, K., (2017). "Physico-mechanical Behaviour of Metamorphic Rocks in Rohtang Tunnel, Himachal Pradesh, India." *ISRM EUROCK, Springer Nature Switzerland AG, v. 50(10),* pp.3013-3030.

Stöcklin, J., (1980). "Geology of Nepal and Its Regional Frame: Thirty-third William Smith Lecture." *Journal of the Geological Society, v. 137(1),* pp.1-34.

Stöcklin, J., and Bhattarai, K., (1977). "Geology of Kathmandu Area and Central Mahabharat Range: Nepal Himalaya." *Department of Mines and Geology, Kathmandu, Nepal,* 86p.

8. APPENDIX

The following tables provide additional data supporting the results discussed in the main text.

Table 1 Stratigraphic units of Central Nepal (Stöcklin and Bhattarai, 1977)

Unit		Formation	Main Lithology	Apparent Thickness (m)	Age
Kathmandu Complex	Bhimphedi Group	Markhu Formation	Marble, schist	1,000	Late Precambrian
		Kulikhani Formation	Quartzite, schist	2,000	Precambrian
		Chisapani Quartzite	White quartzite	400	
		Kalitar Formation	Schist, quartzite	2,000	
		Bhainsedobhan Marble	Marble	800	
		Raduwa Formation	Garnetiferous schist	1,000	
——————————- Mahabharat Thrust (MT) ——————————-					
Nawakot Complex	Upper Nawakot Group	Robang Formation	Phyllite, quartzite	200 – 1,000	Paleozoic
		Malekhu Limestone	Limestone, Dolomite	800	
		Benighat Slate	Slate, argillaceous dolomite	500 – 3,000	

Table 2 Description and classification of ballast samples from the Pandrang Quartzite and the Chisapani Quartzite of the Suparitar-Bhimphedi section, central Nepal lesser Himalaya

Stratig-raphic unit	Sample	Aggregate Type		Physical Characteristics							Petrological Classification				
		Rock/ Gravel/ Sand	Source	Nominal size, mm	Particle Shape	Surface Texture	Colour	Presence of Fines	Coating	Extraneous Materials	Monomictic/ Polymictic	Petrologic Name	Geological Age	Description	Classification
Pandrang Quartzite	P1	Crushed rock	Bedrock	37.5	VA, bladed to equant	Rough	Greenish white	None	None	None	Monomictic	Quartzite	Pre-Camb.	Massive	Crushed Quartzite
	P2	Crushed rock	Bedrock	37.5	VA, bladed to equant	Rough	Dark grey	None	None	None	Monomictic	Quartzite	Pre-Camb.	Massive	Crushed Quartzite
	P3	Crushed rock	Bedrock	37.5	VA, bladed to equant	Rough	Greenish white	None	None	None	Monomictic	Quartzite	Pre-Camb.	Massive	Crushed Quartzite
	P4	Crushed rock	Bedrock	37.5	VA, prolate	Rough	Greenish white	None	None	None	Monomictic	Quartzite	Pre-Camb.	Massive	Crushed Quartzite
	P5	Crushed rock	Bedrock	37.5	VA, prolate	Rough	Greenish white	None	None	None	Monomictic	Quartzite	Pre-Camb.	Massive	Crushed Quartzite
	P6	Crushed rock	Bedrock	37.5	VA, bladed to equant	Rough	Greenish white	None	None	None	Monomictic	Quartzite	Pre-Camb.	Massive	Crushed Quartzite
	P7	Crushed rock	Bedrock	37.5	VA, bladed to equant	Rough	Greenish white	None	None	None	Monomictic	Quartzite	Pre-Camb.	Massive	Crushed Quartzite
	P8	Crushed rock	Bedrock	37.5	VA, prolate	Rough	Greenish white	None	None	None	Monomictic	Quartzite	Pre-Camb.	Massive	Crushed Quartzite
	P9	Crushed rock	Bedrock	37.5	VA, bladed to equant	Rough	Greenish white	None	None	None	Monomictic	Quartzite	Pre-Camb.	Laminated	Crushed Quartzite
	P10	Crushed rock	Bedrock	37.5	VA, bladed to equant	Rough	Greenish white	None	None	None	Monomictic	Quartzite	Pre-Camb.	Massive	Crushed Quartzite
	P11	Crushed rock	Bedrock	37.5	VA, prolate	Rough	Greenish white	None	None	None	Monomictic	Quartzite	Pre-Camb.	Laminated	Crushed Quartzite
	P12	Crushed rock	Bedrock	37.5	VA, bladed to equant	Rough	Greenish white	None	None	None	Monomictic	Quartzite	Pre-Camb.	Massive	Crushed Quartzite
	P13	Crushed rock	Bedrock	37.5	VA, bladed to equant	Rough	Greenish white	None	None	None	Monomictic	Quartzite	Pre-Camb.	Massive	Crushed Quartzite
	P14	Crushed rock	Bedrock	37.5	VA, bladed to equant	Rough	Greenish white	None	None	None	Monomictic	Quartzite	Pre-Camb.	Massive	Crushed Quartzite
	P15	Crushed rock	Bedrock	37.5	VA, bladed to equant	Rough	Greenish white	None	None	None	Monomictic	Quartzite	Pre-Camb.	Massive	Crushed Quartzite
Chisapani Quartzite	C1	Crushed rock	Bedrock	37.5	VA, bladed to equant	Rough	Light greenish grey	None	None	None	Monomictic	Quartzite	Pre-Camb.	Massive	Crushed Quartzite
	C2	Crushed rock	Bedrock	37.5	VA, prolate	Rough	Light greenish grey	None	None	None	Monomictic	Quartzite	Pre-Camb.	Laminated	Crushed Quartzite
	C3	Crushed rock	Bedrock	37.5	VA, bladed to equant	Rough	Light greenish grey	None	None	None	Monomictic	Quartzite	Pre-Camb.	Laminated	Crushed Quartzite
	C4	Crushed rock	Bedrock	37.5	VA, bladed to equant	Rough	Light greenish grey	None	None	None	Monomictic	Quartzite	Pre-Camb.	Laminated	Crushed Quartzite
	C5	Crushed rock	Bedrock	37.5	VA, bladed to equant	Rough	Greenish grey	None	None	None	Monomictic	Quartzite	Pre-Camb.	Massive	Crushed Quartzite
	C6	Crushed rock	Bedrock	37.5	VA, bladed to equant	Rough	Light greenish grey	None	None	None	Monomictic	Quartzite	Pre-Camb.	Laminated	Crushed Quartzite
	C7	Crushed rock	Bedrock	37.5	VA, prolate	Rough	Light greenish grey	None	None	None	Monomictic	Quartzite	Pre-Camb.	Laminated	Crushed Quartzite
	C8	Crushed rock	Bedrock	37.5	VA, bladed to equant	Rough	Light greenish grey	None	None	None	Monomictic	Quartzite	Pre-Camb.	Massive	Crushed Quartzite
	C9	Crushed rock	Bedrock	37.5	VA, bladed to equant	Rough	Greenish grey	None	None	None	Monomictic	Quartzite	Pre-Camb.	Massive	Crushed Quartzite
	C10	Crushed rock	Bedrock	37.5	VA, prolate	Rough	Light greenish grey	None	None	None	Monomictic	Quartzite	Pre-Camb.	Laminated	Crushed Quartzite
	C11	Crushed rock	Bedrock	37.5	VA, bladed to equant	Rough	Light greenish grey	None	None	None	Monomictic	Quartzite	Pre-Camb.	Laminated	Crushed Quartzite
	C12	Crushed rock	Bedrock	37.5	VA, prolate	Rough	Light greenish grey	None	None	None	Monomictic	Quartzite	Pre-Camb.	Laminated	Crushed Quartzite
	C13	Crushed rock	Bedrock	37.5	VA, bladed to equant	Rough	Greenish grey	None	None	None	Monomictic	Quartzite	Pre-Camb.	Laminated	Crushed Quartzite
	C14	Crushed rock	Bedrock	37.5	VA, bladed to equant	Rough	Light greenish grey	None	None	None	Monomictic	Quartzite	Pre-Camb.	Laminated	Crushed Quartzite
	C15	Crushed rock	Bedrock	37.5	VA, bladed to equant	Rough	Light greenish grey	None	None	None	Monomictic	Quartzite	Pre-Camb.	Laminated	Crushed Quartzite

Table 3 Composition of quartzites from the Pandrang Quartzite and the Chisapani Quartzite

Stratigraphic unit	Sample	Mineral constituents, %						Total
		Quartz	Feldspar	Muscovite	Sericite	Biotite	Heavies	
Pandrang Quartzite	P1	90		2	7		1	100
	P2	92		1	6		1	100
	P3	91		2	7		1	100
	P4	91		2	6		1	100
	P5	91		2	6		1	100
	P6	91		2	6	1	1	100
	P7	85		3	5	5		100
	P8	95		1	3		1	100
	P9	91		2	4	2	1	100
	P10	85		4	5	1	2	100
	P11	89	1	4	5		1	100
	P12	92		2	5		1	100
	P13	91		2	6		1	100
	P14	83		7	5	4	1	100
	P15	86	1	2	4	5	1	100
Chisapani Quartzite	C1	86		5	4	4	1	100
	C2	85		5	3	4	2	100
	C3	86		3	5	5	1	100
	C4	91		5	3		1	100
	C5	90		6	3		1	100
	C6	87		6	4		3	100
	C7	86		3	3	6	2	100
	C8	89		6	3	1	1	100
	C9	88		4	3	4	1	100
	C10	90		4	3	2	1	100
	C11	86		5	3	5	1	100
	C12	88		5	3	3	1	100
	C13	88		4	4	3	1	100
	C14	90		4	3	3	1	100
	C15	87		5	4	3	1	100

Table 4 Density, specific gravity, and water absorption of the ballasts from the Pandrang Quartzite and the Chisapani Quartzite

Stratigraphic unit	Sample number	Mass of Oven-dry sample in air (Kg), A	Mass of saturated surface dry (SSD) wt. in air, (Kg), B	Mass of saturated sample in water (Kg), C	Specific Gravity, G = B/(B-C)	Oven-Dry Density, D = 997.5 {A/(B-C)} (Kg/m^3)	Water absorption, WA ={(B-A)/A}100, %
Pandrang Quartzite	P1	2.020	2.025	1.270	2.68	2669	0.25
	P2	2.065	2.075	1.30	2.68	2658	0.48
	P3	2.020	2.030	1.245	2.59	2567	0.50
	P4	2.020	2.030	1.250	2.60	2583	0.50
	P5	2.025	2.030	1.260	2.64	2623	0.25
	P6	2.055	2.070	1.285	2.64	2611	0.73
	P7	2.000	2.010	1.250	2.64	2625	0.50
	P8	2.055	2.060	1.270	2.61	2595	0.24
	P9	2.010	2.020	1.250	2.62	2604	0.50
	P10	2.005	2.010	1.245	2.63	2614	0.25
	P11	2.055	2.065	1.295	2.68	2662	0.49
	P12	2.035	2.040	1.270	2.65	2636	0.25
	P13	2.020	2.035	1.225	2.51	2488	0.74
	P14	2.085	2.100	1.265	2.51	2491	0.72
	P15	2.045	2.060	1.240	2.51	2488	0.73
Chisapani Quartzite	C1	2.02	2.03	1.25	2.60	2583	0.25
	C2	2.06	2.07	1.26	2.54	2521	0.49
	C3	2.04	2.05	1.27	2.61	2586	0.74
	C4	2.06	2.07	1.28	2.63	2611	0.49
	C5	2.08	2.09	1.29	2.62	2604	0.48
	C6	2.05	2.06	1.28	2.64	2622	0.49
	C7	2.08	2.09	1.29	2.62	2604	0.48
	C8	2.09	2.10	1.27	2.53	2506	0.72
	C9	2.06	2.06	1.31	2.75	2733	0.24
	C10	2.05	2.07	1.28	2.61	2582	0.98
	C11	2.02	2.03	1.25	2.59	2560	0.74
	C12	2.09	2.11	1.30	2.61	2584	0.96
	C13	2.01	2.03	1.26	2.63	2597	1.00
	C14	2.07	2.09	1.30	2.66	2630	0.72
	C15	2.01	2.03	1.25	2.60	2570	1.00

Table 5 Bulk density and %void of quartzite ballasts

Stratigraphic unit	Sample	Mass of ballast (Kg)	Volume of bucket (m^3)	Bulk density (Kg/m^3)	*Void (%)
Pandrang Quartzite	P1	2.98	0.00221	1348	49
	P2	2.545	0.00221	1152	56
	P3	2.845	0.00221	1287	51
	P4	2.79	0.00221	1262	52
	P5	2.935	0.00221	1328	50
	P6	2.79	0.00221	1262	52
	P7	2.87	0.00221	1299	51
	P8	2.92	0.00221	1321	50
	P9	2.67	0.00221	1208	54
	P10	2.79	0.00221	1262	52
	P11	3.03	0.00221	1371	48
	P12	2.565	0.00221	1161	56
	P13	2.695	0.00221	1219	54
	P14	2.795	0.00221	1265	52
	P15	2.95	0.00221	1335	50
Chisapani Quartzite	C1	3.14	0.00221	1421	46
	C2	2.86	0.00221	1292	51
	C3	2.83	0.00221	1281	52
	C4	3.19	0.00221	1441	46
	C5	2.89	0.00221	1305	51
	C6	2.98	0.00221	1348	49
	C7	2.92	0.00221	1319	50
	C8	2.97	0.00221	1344	49
	C9	2.79	0.00221	1260	52
	C10	2.79	0.00221	1262	52
	C11	2.92	0.00221	1319	50
	C12	3.03	0.00221	1369	48
	C13	2.92	0.00221	1319	50
	C14	3.01	0.00221	1362	49
	C15	2.93	0.00221	1324	50

*Void = {(2.65 x 998)-BD}/(2.65 x 998)}*100

Table 6 Results of Point-load strength index and UCS of quartzite ballasts

Stratigraphic unit	Location	W1, cm	W2, cm	Wavg, mm	D1, cm	D2, cm	Davg, mm	$De^2 = 4A/\pi$, mm^2	Load, P, KN	$I_s = P/De^2$, Mpa	$F = (De/50)^{0.45}$	$I_{s(50)} = I_s . F$, Mpa	$I_{s(50)}$, Mpa	$UCS = 24*I_{s(50)}$, Mpa	*Remarks
Pandrang Quartzite	P1	4.90	5.10	50.00	4.40	4.40	44.00	2800.76	23.6	8.41	1.026	8.63	4.31	207	Very strong
		4.70	4.80	47.50	4.40	4.90	46.50	2811.90	18.4						
	P2	4.10	4.90	45.00	3.40	4.20	38.00	2176.96	8.6	3.94	0.969	3.82	1.91	92	Strong
		3.80	4.20	40.00	3.80	4.00	39.00	1986.00	11.5						
	P3	4.80	5.00	49.00	3.70	3.80	37.50	2339.27	16.5	7.06	0.985	6.96	3.48	167	Very strong
		4.50	4.70	46.00	4.00	4.60	43.00	2518.14	12.5						
	P4	4.10	4.50	43.00	4.00	4.10	40.50	2217.06	9.2	4.16	0.973	4.05	2.03	97	Strong
		3.70	4.50	41.00	3.80	4.20	40.00	2087.84	26.4						
	P5	4.20	4.60	44.00	3.90	4.10	40.00	2240.61	14.7	6.57	0.976	6.41	3.20	154	Very strong
		4.70	5.20	49.50	3.00	3.20	31.00	1953.53	31.8						
	P6	3.90	4.50	42.00	3.00	3.20	31.00	1657.54	5.3	3.20	0.912	2.92	1.46	70	Strong
		4.10	4.30	42.00	3.20	4.00	36.00	1924.89	12.3						
	P7	5.00	5.20	51.00	3.20	3.60	34.00	2207.51	9.8	4.43	0.972	4.31	2.15	103	Very strong
		4.10	5.80	49.50	3.50	4.40	39.50	2489.18	5.2						
	P8	4.30	4.70	45.00	2.80	3.10	29.50	1690.01	9.2	5.46	0.916	5.00	2.50	120	Very strong
		3.3	3.70	35.00	3.40	3.40	34.00	1514.96	28.4						
	P9	4.20	5.00	46.00	3.10	4.10	36.00	2108.21	6.5	3.09	0.962	2.98	1.49	71	Strong
		5.20	5.40	53.00	3.20	3.60	34.00	2294.08	13.5						
	P10	4.00	4.40	42.00	3.10	3.50	33.00	1764.48	7.6	4.30	0.925	3.98	1.99	95	Strong
		2.90	5.20	40.50	3.10	2.50	28.00	1443.67	15.0						
	P11	3.70	4.30	40.00	3.40	3.50	34.50	1756.84	10.4	5.94	0.924	5.48	2.74	132	Very strong
		3.80	3.90	38.50	3.30	3.50	34.00	1666.45	4.4						
	P12	4.00	4.60	43.00	3.80	4.60	42.00	2299.17	12.2	5.31	0.981	5.22	2.61	125	Very strong
		4.00	4.60	43.00	3.20	3.80	35.00	1915.98	7.8						
	P13	4.00	4.40	42.00	3.10	4.50	38.00	2031.83	7.4	3.66	0.954	3.49	1.75	84	Strong
		4.30	4.50	44.00	3.10	3.30	32.00	1792.49	6.5						
	P14	4.00	4.80	44.00	3.40	3.80	36.00	2016.55	10.6	5.25	0.953	5.00	2.50	120	Very strong
		4.70	5.10	49.00	3.00	3.20	31.00	1933.80	11.1						
	P15	4.00	4.80	44.00	3.40	3.80	36.00	2016.55	13.4	6.62	0.953	6.31	3.15	151	Very strong
		3.50	4.90	42.00	2.00	3.80	29.00	1550.60	11.9						
Chisapani Quartzite	C1	3.90	3.70	38.00	4.40	3.20	38.00	1838.32	11.72	6.38	0.933	5.95	2.97	143	Very strong
		4.60	4.20	44.00	3.20	3.00	31.00	1736.47	5.32						
	C2	4.50	3.90	42.00	3.90	3.10	35.00	1871.42	8.25	4.41	0.937	4.13	2.07	99	Strong
		4.60	3.80	42.00	4.00	3.40	37.00	1978.36	9.75						
	C3	3.90	3.50	37.00	4.20	2.20	32.00	1507.32	11.43	7.58	0.892	6.77	3.38	162	Very strong
		5.00	3.60	43.00	3.40	3.30	33.50	1833.86	14.55						
	C4	5.00	4.30	46.50	3.50	3.30	34.00	2012.73	29.69	14.75	0.952	14.05	7.02	337	Extremely stron
		4.70	3.90	43.00	4.40	3.80	41.00	2244.43	9.13						
	C5	4.80	4.20	45.00	3.80	3.60	37.00	2119.67	15.07	7.11	0.964	6.85	3.43	164	Very strong
		4.40	3.40	39.00	3.90	3.50	37.00	1837.05	19.01						
	C6	4.00	3.00	35.00	3.50	3.30	34.00	1514.96	12.22	8.07	0.893	7.21	3.60	173	Very strong
		4.10	3.80	39.50	4.20	3.40	38.00	1910.88	13.89						
	C7	4.40	4.20	43.00	3.80	3.20	35.00	1915.98	8.26	4.31	0.942	4.06	2.03	97	Strong
		3.60	3.50	35.50	3.60	3.40	35.00	1581.80	7.30						
	C8	4.20	3.80	40.00	4.00	3.40	37.00	1884.15	7.35	3.90	0.938	3.66	1.83	88	Strong
		4.50	3.90	42.00	4.10	3.40	37.50	2005.09	10.52						
	C9	4.30	4.00	41.50	3.90	3.30	36.00	1901.97	8.82	4.64	0.940	4.36	2.18	105	Very strong
		5.20	4.70	49.50	4.30	3.90	41.00	2583.70	12.60						
	C10	4.40	4.00	42.00	3.20	3.00	31.00	1657.54	7.92	4.78	0.912	4.36	2.18	105	Very strong
		4.90	4.70	48.00	4.60	4.40	45.00	2749.84	9.28						
	C11	4.20	4.10	41.50	4.10	3.90	40.00	2113.30	10.85	5.13	0.963	4.94	2.47	119	Very strong
		4.80	4.50	46.50	3.70	3.60	36.50	2160.73	2.30						
	C12	4.50	4.50	45.00	3.90	3.60	37.50	2148.31	2.35	1.09	0.966	1.06	0.53	25	Medium strong
		4.50	3.70	41.00	4.00	3.70	38.50	2009.55	5.50						
	C13	5.00	4.20	46.00	3.10	2.90	30.00	1756.84	7.82	4.45	0.924	4.11	2.06	99	Strong
		4.40	3.50	39.50	3.70	3.50	36.00	1810.31	10.05						
	C14	4.40	3.80	41.00	3.90	4.00	39.50	2061.74	3.50	1.70	0.958	1.63	0.81	39	Medium strong
		3.90	3.40	36.50	3.50	3.40	34.50	1603.12	8.85						
	C15	3.70	3.80	37.50	3.90	3.30	36.00	1718.65	9.72	5.66	0.919	5.20	2.60	125	Very strong
		3.80	4.10	39.50	3.60	3.80	37.00	1860.60	4.52						
	*Brown (1981): 0.25-1 MPa= extremely weak; 1-5.0 MPa= very weak; 5.0-25 MPa = weak; 25-50 MPa= medium strong rock; 50-100 MPa= strong; 100-250 MPa= very strong; >250 MPa extremely strong														

Table 7 Test results of AIV and ACV of the quartzite samples from the Pandrang Quartzite and the Chispani Quartzite

Stratigraphic unit	Sample	Initial Weight (gm)	Retained Weight from 2.36 sieve (gm)	Aggregate Impact Value, AIV (%)	Intial Weight (Kg)	Retained Weight from 2.36 sieve (Kg)	Aggregate Crushing Value, ACV (%)
Pandrang Quartzite	P1	515	440	15	3.01	2.339	22
	P2	515	390	24	3.016	2.183	28
	P3	515	430	17	3.004	2.252	25
	P4	515	410	20	3.01	2.262	25
	P5	515	435	16	3.008	2.244	25
	P6	515	425	17	3.005	2.289	24
	P7	520	425	18	3.009	2.255	25
	P8	520	425	18	3.007	2.341	22
	P9	515	450	13	3.011	2.337	22
	P10	515	450	13	3.014	2.371	21
	P11	510	405	21	3.012	2.355	22
	P12	510	410	20	3.019	2.311	23
	P13	510	425	17	3.011	2.298	24
	P14	505	390	23	3.011	2.119	30
	P15	520	415	20	3.006	2.134	29
Chisapani Quartzite	C1	510	420	18	3.01	2.404	20
	C2	520	420	19	3.012	2.221	26
	C3	505	405	20	3.014	2.232	26
	C4	505	435	14	3.011	2.331	23
	C5	510	415	19	3.013	2.205	27
	C6	510	390	24	3.018	2.079	31
	C7	520	385	26	3.013	2.127	29
	C8	515	395	23	3.015	1.963	35
	C9	515	440	15	3.007	2.252	25
	C10	505	340	33	3.01	1.913	36
	C11	515	395	23	3.02	2.248	26
	C12	520	350	33	3.019	1.912	37
	C13	530	415	22	3.008	2.097	30
	C14	510	375	26	3.01	2.089	31
	C15	515	340	34	3.008	1.859	38

Table 8 Results of Slake Durability Index of quartzite samples from the Pandrang Quartzite and the Chisapani Quartzite

Stratigraphic unit	Sample	Initial wt. (g)	Initial Oven-dry wt. before the 1st cycle (g)	Oven-dry wt. after 1st cycle (g)	Oven-dry wt. after 2nd cycle (g)	Oven-dry wt. after 3rd cycle (g)	Oven-dry wt. after 4th cycle (g)	Oven-dry wt. after completing the 5th cycle (g)	*I_{d2} (%)		I_{d5} (%)		
Pandrang Quartzite	P1	505	505	505	505	505	505	505	100	VHD	I	100	VHD
	P2	545	545	540	540	540	535	535	99	VHD	I	98	VHD
	P3	525	525	525	525	525	520	520	100	VHD	I	99	VHD
	P4	505	505	505	500	500	500	500	99	VHD	I	99	VHD
	P5	505	505	505	505	505	500	500	100	VHD	I	99	VHD
	P6	555	555	550	550	545	545	545	99	VHD	I	98	VHD
	P7	550	550	545	545	545	545	540	99	VHD	I	98	VHD
	P8	560	555	555	555	550	550	550	100	VHD	I	99	VHD
	P9	505	505	500	500	500	500	500	99	VHD	I	99	VHD
	P10	555	550	550	550	550	545	545	100	VHD	I	99	VHD
	P11	545	545	540	535	535	535	535	98	VHD	I	98	VHD
	P12	545	545	545	540	540	540	540	99	VHD	I	99	VHD
	P13	555	555	550	550	550	550	550	99	VHD	I	99	VHD
	P14	560	560	555	555	555	555	550	99	VHD	I	98	VHD
	P15	545	545	540	540	540	535	535	99	VHD	I	98	VHD
Chisapani Quartzite	C1	550	550	550	545	545	545	545	99	VHD	I	99	VHD
	C2	525	525	525	520	520	520	520	99	VHD	I	99	VHD
	C3	570	570	565	560	560	560	560	98	VHD	I	98	VHD
	C4	540	540	540	540	540	540	540	100	VHD	I	100	VHD
	C5	505	505	500	500	500	500	495	99	VHD	I	98	VHD
	C6	520	520	515	515	515	515	510	99	VHD	I	98	VHD
	C7	520	520	515	515	515	515	515	99	VHD	I	99	VHD
	C8	530	530	530	530	525	525	525	100	VHD	I	99	VHD
	C9	535	535	530	530	530	530	530	99	VHD	I	99	VHD
	C10	585	585	580	580	575	575	575	99	VHD	I	98	VHD
	C11	530	530	530	530	525	525	525	100	VHD	I	99	VHD
	C12	540	535	530	525	520	520	520	98	VHD	I	97	HD
	C13	530	530	530	525	525	525	520	99	VHD	I	98	VHD
	C14	540	540	540	535	535	535	530	99	VHD	I	98	VHD
	C15	545	545	535	535	535	530	530	98	VHD	I	97	HD

* Slake Durability Classification (Goodman, 1980): I_{d2}: >98% very high durability (VHD); 95-98% high durability (HD);

85-95 medium high durability; 60-85 medium durability; 30-60 low durability; <30 very low durability, and Deterioration Type.

Table 9 Results of Los Angeles abrasion test of quartzite samples from the Pandrang Quartzite and the Chisapani Quartzite

Stratigraphic unit	Sample	Initial mass passing 50 mm and retained on 37.5 sieves (Kg)	Initial mass of the sample passing 37.5 mm and retained on 25 mm sieves (Kg)	Total mass of test sample (Kg)	Wt. retained on 1.7 mm sieve after 1000 revolution (Kg)	Loss in wt. (Kg)	LAAV (%)
Pandrang Quartzite	P1	5.060	5.035	10.095	8.495	1.600	16
	P2	5.015	5.035	10.050	7.600	2.450	24
	P3	5.060	5.040	10.100	7.285	2.815	28
	P4	5.055	5.100	10.155	7.345	2.810	28
	P5	5.040	5.135	10.175	7.725	2.450	24
	P6	5.010	5.010	10.020	6.765	3.255	32
	P7	5.120	5.070	10.190	7.000	3.190	31
	P8	5.010	5.025	10.035	7.655	2.380	24
	P9	5.060	5.035	10.095	7.070	3.025	30
	P10	5.090	5.050	10.140	7.830	2.310	23
	P11	5.030	5.065	10.095	7.765	2.330	23
	P12	5.06	5.115	10.175	6.725	3.450	34
	P13	5.045	5.070	10.115	6.355	3.760	37
	P14	5.125	5.065	10.190	7.295	2.895	28
	P15	5.14	5.075	10.215	7.725	2.490	24
Chisapani Quartzite	C1	5.10	5.05	10.15	7.56	2.590	26
	C2	5.03	5.02	10.05	6.82	3.225	32
	C3	5.05	5.07	10.11	6.93	3.185	32
	C4	5.07	5.05	10.11	7.85	2.260	22
	C5	5.06	5.05	10.11	7.70	2.405	24
	C6	5.02	5.05	10.07	6.76	3.305	33
	C7	5.11	5.06	10.17	6.73	3.445	34
	C8	5.08	5.03	10.10	5.62	4.480	44
	C9	5.02	5.01	10.03	7.77	2.265	23
	C10	5.10	5.09	10.18	5.93	4.250	42
	C11	5.06	5.11	10.16	5.63	4.535	45
	C12	5.01	5.02	10.03	5.15	4.875	49
	C13	5.05	5.03	10.08	6.73	3.350	33
	C14	5.06	5.05	10.11	5.95	4.155	41
	C15	5.08	5.06	10.13	5.27	4.860	48

Table 10 Results of sulphate soundness test of quartzite samples from the Pandrang Quartzite and the Chisapani Quartzite

Stratigraphic unit	Sample	Initial wt. (Kg)	1st cycle: wt. after immersion in $MgSO_4$ and drying in the oven (Kg)	2nd cycle: wt. after immersion in $MgSO_4$ and drying in the oven (Kg)	3rd cycle: wt. after immersion in $MgSO_4$ and drying in the oven (Kg)	4th cycle: wt. after immersion in $MgSO_4$ and drying in the oven (Kg)	5th cycle: wt. after immersion in $MgSO_4$ and drying in the oven (Kg)	wt. after washing with $BaCl_2$ solution (Kg)	SSV%
Pandrang Quartzite	P1	2.020	2.020	2.025	2.025	2.025	2.025	2.020	0.00
	P2	2.065	2.070	2.075	2.075	2.065	2.075	2.065	0.00
	P3	2.020	2.025	2.025	2.025	2.025	2.025	2.020	0.00
	P4	2.020	2.025	2.030	2.030	2.030	2.030	2.020	0.00
	P5	2.025	2.025	2.030	2.030	2.030	2.030	2.025	0.00
	P6	2.055	2.060	2.060	2.065	2.065	2.065	2.055	0.00
	P7	2.000	2.005	2.010	2.010	2.010	2.010	2.000	0.00
	P8	2.045	2.050	2.050	2.045	2.050	2.050	2.045	0.00
	P9	2.010	2.015	2.015	2.015	2.020	2.020	2.010	0.00
	P10	2.005	2.010	2.015	2.010	2.005	2.010	2.005	0.00
	P11	2.055	2.060	2.065	2.065	2.060	2.060	2.050	0.24
	P12	2.035	2.035	2.035	2.035	2.035	2.035	2.030	0.25
	P13	2.020	2.025	2.025	2.035	2.025	2.025	2.020	0.00
	P14	2.085	2.090	2.095	2.090	2.095	2.100	2.085	0.00
	P15	2.045	2.050	2.060	2.060	2.060	2.060	2.045	0.00
Chisapani Quartzite	C1	2.020	2.020	2.025	2.025	2.025	2.020	2.015	0.25
	C2	2.060	2.065	2.065	2.065	2.065	2.065	2.060	0.00
	C3	2.035	2.040	2.045	2.045	2.040	2.045	2.020	0.74
	C4	2.060	2.060	2.060	2.060	2.060	2.070	2.060	0.00
	C5	2.075	2.800	2.085	2.075	2.075	2.080	2.075	0.00
	C6	2.055	2.060	2.060	2.060	2.065	2.065	2.055	0.00
	C7	2.080	2.080	2.080	2.080	2.080	2.085	2.080	0.00
	C8	2.090	2.090	2.090	2.095	2.095	2.095	2.090	0.00
	C9	2.050	2.055	2.055	2.055	2.030	2.040	2.050	0.00
	C10	2.045	2.060	2.055	2.060	2.065	2.060	2.045	0.00
	C11	2.015	2.025	2.025	2.020	2.020	2.025	2.015	0.00
	C12	2.090	2.100	2.105	2.100	2.090	2.095	2.080	0.48
	C13	2.010	2.015	2.020	2.020	2.015	2.020	2.010	0.00
	C14	2.070	2.080	2.080	2.080	2.080	2.080	2.070	0.00
	C15	2.010	2.020	2.020	2.020	2.020	2.020	2.005	0.25

Table 11 Comparison of the Quartzites with AREMA and BR specification

	Test	Procedure	AREMA (2010)	BS EN 13450 (BS 2013)	Pandrang Quartzite	Chisapani Quartzite
Physical Properties	Density (Specific Gravity)	ASTM C 127	<2600 kg/m^3	-	2488 -2669 kg/m^3 (2.54 to 2.70)	2521- 2733 kg/m^3 (2.53 to 2.75)
	Water Absorption (%WA)	ASTM C127	1 to 2%	-	0.24 to 0.74%	0.24% to 1.00%
	Bulk density	ASTM C127	>1120 kg/m^3	-	1152- 1371kg/m^3	1260- 1441 kg/m^3
Mechanical Properties	Point Load Strength Index ($I_{s(50)}$)	ASTM D5731–02	Dry>1200 kg Wet> 800 kg		72 to 207 MPa	19 MPa to 70 MPa
	Aggregate Impact Value (AIV)	BS 812- 112	-	<22 %	13 % to 24%	14% to 34%.
	Aggregate Crushing Value (ACV)	BS 812- 110	-	<22 %	21 to 30%	21% to 30%.
Durability	Slake Durability	ASTM D 4644-87	Not allocated	Not allocated	98 to 100%	97% to 100%
	Los Angeles Abrasion Value (LAAV)	ASTM C535	35% max.	25%	21% to 30%	22% to 49%.
	Sulfate Soundness Value	ASTM C88	< 5% (5-cycles)	1% Nacl-10 cycles	0 to 0.48%	0 to 0.24%.